AN EXAMPLE OF LIGNOCELLULOSIC WASTE REUSE IN TWO CONSECUTIVE STEPS: SORPTION OF CONTAMINANTS AND ENZYMATIC HYDROLYSIS

VIVIANE DA SILVA[1], JUAN B. LÓPEZ-SOTELO[1], ADRIANA CORREA-GUIMARAES[1],
SALVADOR HERNÁNDEZ-NAVARRO[1], MERCEDES SÁNCHEZ-BÁSCONES[1],
LUIS M. NAVAS-GRACIA[1], PABLO MARTÍN-RAMOS[2,*] and
JESÚS MARTÍN-GIL[1]

[1] Agricultural and Forestry Engineering Department, ETSIIAA, University of Valladolid, Avenida de Madrid 44, 34004 Palencia, Spain
[2] Department of Agricultural and Environmental Sciences, Higher Polytechnic School of Huesca, Universidad de Zaragoza, Carretera de Cuarte s/n, 22071, Huesca, Spain
* pmr@unizar.es

In this study an example of the reuse and revalorization of lignocellulosic waste from carnauba palm (*Copernicia prunifera*) leaves, macauba palm (*Acrocomia aculeata*) endocarp (shell) and European stone pine (*Pinus pinea*) nut shell is presented for the first time. The physical-chemical adsorption of Rhodamine B (RhB) dye for the different materials is studied in detail, together with the thermodynamic feasibility and the spontaneous and endothermic nature of the biosorption process. Subsequently, the production of total reducing sugars (TRS) is compared by enzymatic hydrolysis (before and after the adsorption process of the RhB pollutant), confirming the viability of TRS production in all cases, with yields ranging from 65.9% for pine nut shell (after adsorption) to 74.9% for the carnauba endocarp and to 84.0% for carnauba leaves (before adsorption). Hence the use of lignocellulosic materials as adsorbents does not preclude their ulterior reuse for obtaining fermentable sugars by enzymatic hydrolysis.

Keywords: carnauba, enzymatic hydrolysis, fermentable sugars, lignocellulosic residues, macauba, pine nut shell, reuse

INTRODUCTION

Lignocellulosic biomass consists of three main components, namely cellulose, hemicellulose and lignin. Cellulose and hemicellulose are densely packed and covered by layers of lignin, which protect them from enzymatic hydrolysis. Therefore it is necessary to have a pre-treatment stage in order to cause the rupture of lignin layers, making the cellulose and hemicellulose more accessible to the enzymes.[1-3]

Chemical pre-treatments have serious disadvantages, such as the production of harmful by-products that interfere with the activity and removal of the enzymes. In comparison to chemical methods, biological pre-treatment is deemed as a safe and environmentally-friendly method to break down lignin from lignocellulose.[4] The enzymatic hydrolysis or saccharification aims to produce depolymerisation of cellulose and hemicellulose to hexose and pentose, two carbohydrates which are considered to have significant potential for biofuel production.[5]

In the work presented herein, three agroforestry residues have been chosen to assess the adsorption of contaminants: (i) leaves from carnauba palm (*Copernicia prunifera* (Mill.) H.E.Moore), used for wax production;[6] (ii) endocarp or shell from macauba palm (*Acrocomia aculeata* (Jacq.) Lodd. ex Mart.), used for the production of biodiesel;[7] and (iii) European stone pine nut shell (*Pinus pinea* L.), which is used for the production of biogas. The approach of this research is an integrated study of the utilization of lignocellulosic wastes with a twofold purpose: firstly, to make use of them as adsorbents for the removal of toxic or hazardous dyes in liquid effluents and, subsequently (once the dye has been adsorbed), to reuse them for sugars production by saccharification or enzymatic hydrolysis. Thus, the TRS yields have first been determined for the bare lignocellulosic materials and have then been compared with those attained after dye adsorption, assessing their viability for the production of these biofuel precursors.

EXPERIMENTAL

Characterization of lignocellulosic waste

Carnauba palm leaves from Ceará (Brazil), macauba palm endocarp from Minas Gerais (Brazil) and European stone pine nut shell from Valladolid (Spain) were used as lignocellulosic raw materials. The materials were dried in an oven (105 ºC, 24 hours) and were subsequently grounded and sieved through a 0.5 mm mesh.

The pH at point zero charge (pH_{PZC}) was determined by the solids addition method[8] using a 0.01 M KNO_3 solution. The concentrations of acidic and basic surface functional groups were determined by Boehm titration method.[9] C, H and N contents were measured using a Leco CHN-600 Elemental Analyzer. The oxygen content was calculated by subtraction. The adsorption capacity was determined using methylene blue (MB) index[10] and the iodine absorption index, which was measured according to ASTM D4607-94 norm.

Accessible surface area measurement techniques can be conducted on the substrate either its dry state (physical gas adsorption/desorption, BET surface determination) or in its wet state (e.g., solute exclusion, iodine index or methylene blue index). In the former, an inert gas, mostly nitrogen, is adsorbed on the surface of a solid material. This occurs on the outer surface and, in case of porous materials, also on the surface of pores. Adsorption of nitrogen at a temperature of 77 K leads to a so-called adsorption isotherm, sometimes referred to as BET isotherm. Nonetheless, gas adsorption methods have limitations: they typically result in an over-estimation of the material accessibility due to the fact that the molecular size of the probe gas is much smaller than cellulase enzymes, and require a prior drying of the substrate, which makes them typically less effective in determining the pore volume due to the fact that water removal from non-rigid porous materials could produce partial irreversible collapse of pores.[11] On the other hand, some of the techniques capable of measuring the substrate in its wet state, such as the solute exclusion,[12] require significant experiment time and only measure the interior surface of the cellulose.[13] Consequently, in this study we have resourced to a combination of both types of measurements: the pore structure of samples has been characterized in their dry state by nitrogen adsorption at 77 K with an accelerated surface area and porosimetry system Micromeritics ASAP 2020 (prior to analysis, samples were degassed for 2 h under vacuum at 393 K and were then transferred to the analysis system where they were cooled in liquid nitrogen) and in their wet state by iodine and methylene blue indices,[14] mentioned above, since the adsorbents are used in an aqueous system.

The surface morphology of the raw materials was observed with the aid of scanning electron microscopy (SEM) in an ESEM FEI Quanta 200F. Samples were coated with gold and observed using a 20 kV voltage.

Rhodamine B adsorption experiments

Batch adsorption experiments were used to investigate the adsorption of Rhodamine B in the different lignocellulosic materials. All adsorption experiments were carried out with a 2 g·L^{-1} adsorbent concentration, and the amount adsorbed per biosorbent mass unit was expressed in mg·g^{-1}. In order to determine the effect on the adsorption of the variations in the initial Rhodamine-B concentration (1-35 mg·L^{-1}), tests were carried out at 25 °C for 120 min. These tests were repeated at 35 ºC and 45 ºC so as to assess the effect of temperature variation in dye adsorption for the materials under study. The influence of contact time was investigated using the same initial dye concentration, $C_o = 5$ mg·L^{-1}, for carnauba leaves and pine nut shell, and $C_o = 20$ mg·L^{-1} for macauba endocarp, varying the contact time from 5 to 240 min. After the biosorption process, the solutions were filtered and dye concentration was measured with a Hitachi U-2001 spectrophotometer (at 553 nm). After the adsorption, the different lignocellulosic materials used as biosorbents were filtrated, washed and dried. These materials were subsequently used for the enzymatic hydrolysis assays.

It should be clarified that only ca. 3% of the adsorbed dye was desorbed during aforementioned washing process with distilled water, on the basis of Rhodamine B concentration measurements conducted for the washing solution, in good agreement with Zahir et al.[15]

Saccharification or enzymatic hydrolysis

Saccharification or enzymatic hydrolysis was performed for the aforementioned lignocellulosic materials before RhB adsorption: carnauba leaves (C), macauba shell (M) and pine nut shell (P); and after RhB adsorption: carnauba leaves (C_R), macauba shell (M_R) and pine nut shell (P_R). No pretreatment was conducted, although carrying out a pretreatment of the lignocellulosic materials would be needed in order to achieve reasonable rates in extensive conversion by enzymatic hydrolysis.[16] For the enzymatic hydrolysis, 0.5 g of sample was immersed in a 10 mL citrate buffer (0.05 M, pH 5) solution with a cocktail of six enzymes. Six laboratory grade enzyme solutions from Novozymes were used: NS22086 (cellulase) (200 µL enzyme per 1 g of dry biomass), NS 22118 (β-glucosidase, arabinase and β-glucanase) (40 µL enzyme per 1 g of dry biomass), NS22083 (xylanase) (40 µL enzyme per 1 g of dry biomass), NS 22002 (β-glucanase and xylanase) (40 µL enzyme per 1 g of dry biomass), NS22119 (cellulase, hemicellulase, pectinase and xylanase) (40 µL enzyme per 1 g of dry biomass) and NS22035 (glucoamylase) (40 µL enzyme per 1 g of dry biomass). The declared activity for each enzyme was 1000 endoglucanase units (EGU)/g, 250 cellobiase units (CBU)/g, 100 fungal β-glucanase units (FBG)/g, 13700 polygalacturonase units (PGU)/g, 2500 fungal xylanase units (FXU-S)/g, 45 FBG/g, and 750 PGU.[17] The

incubation time was 72 h at 50 °C, in a Heidoph Reax 2 rotary shaker. All experiments were performed in triplicate and the reported values correspond to the average.

Analytical methods

The composition of the liquid phase resulting from the enzymatic hydrolysis of carnauba leaves (C_{EH}), carnauba leaves with RhB (C_{REH}), macauba endocarp (M_{EH}), macauba endocarp with RhB (M_{REH}), pine nut shell (P_{EH}) and pine nut shell with RhB (P_{REH}) was determined using a Metrohm 850 Professional IC ion chromatograph with ultrafiltration system, which allowed us to determine the concentration of the various monosaccharides (glucose, xylose, galactose, fructose and arabinose). With regard to the content of total reducing sugars (TRS), the 3,5-dinitrosalicylic acid method (DNS) methodology proposed by Miller[18] was used. The specific concentration of TRS is defined as the amount of TRS obtained from the hydrolysis per mass unit of dry material. The TRS yield was obtained from the following equation:

$$[TRS]\ (\%) = \frac{\text{Concentration of TRS } (g \cdot L^{-1})}{\text{Initial biomass concentration } (g \cdot L^{-1})} \times 100$$

The HMF and furfural values were determined according to the methodology proposed by Chi *et al.*[19] using UV spectrophotometry at 277 and 285 nm, respectively. For the measurement of soluble lignin, a standard curve was prepared using soluble lignin supplied by Sigma Aldrich, and its concentration was determined with a UV-visible spectrophotometer at 280 nm.

RESULTS AND DISCUSSION
Biomass characterization

The physicochemical properties of the materials are described in Table 1. The C, H, N and O percentages for the different materials were similar to those reported for other lignocellulosic materials,[21] showing an elevated content of C and O. The determination of acidic and basic groups on the surface of the samples showed a prevalence of acidic groups (carboxylic, phenolic, lactones and carbonyls) over basic groups, so the surface of the materials was acidic. This acidic nature was also confirmed with the values obtained from pH_{PZC}.

As noted above, the iodine number and the methylene blue number are related to the porosity of the starting material in its wet state.[14] Determining the methylene blue number allows to know the material's ability to adsorb aromatic dyes and indicates the macroporosity of the material under study, while the iodine number is related to micro and mesopores. According to Table 1, the methylene blue values were greater than the iodine values for all the lignocellulosic materials, so it can be inferred that the materials had a larger amount of macropores and a smaller amount of meso/micropores. While this predominance of macropores over meso- and micropores was confirmed with the dry state porosity measurement techniques, namely nitrogen adsorption isotherms, for macauba endocarp and pine nut shell, a contradictory predominance of mesopores was observed for carnauba leaves. These differences between the wet and dry porosity results can be ascribed to hydration phenomena (mentioned above), which lead to an increase both in pore and surface area, particularly marked in the case of carnauba since it was the material with the highest cellulose content.

The carnauba leaf was the residue with the highest values for both indices, 978.37 mg·L^{-1}·g^{-1} and 523.86 mg·g^{-1} for the MB number and iodine number, respectively. These data were in agreement with the total pore volume and the average pore diameter, which were much lower in the carnauba leaves than in the macauba or the pine nut shells. Therefore, we can conclude that there was a predominance of mesopores in the carnauba leaves and of macropores in the macauba and pine nut shells. The analysis conducted with ImageJ software on the scanning electron microscopy (SEM) micrographs also supported that the macauba and pine nut shells were materials with a higher amount of macropores on the surface (see Figure 1). It is worth noting that the presence of macropores in the raw materials - without any chemical, mechanical or thermal pretreatment- was much lower than in the treated samples or in activated carbons. The Brunauer, Emmett and Teller (BET) area confirmed that the tested natural lignocellulosic materials had a very small surface area (from 0.60 to 0.86) m^2·g^{-1} in comparison to activated carbon (3000 m^2·g^{-1}), and therefore the former would be less suitable for the physical adsorption of pollutants. However, the lower porosity of these natural materials *versus* carbonaceous ones from the standpoint of physical adsorption mechanisms is offset by other chemical mechanisms (*e.g.*, valence forces through sharing or exchange of electrons between adsorbent and adsorbate),[22] which can make them viable for the adsorption of pollutants.

Effects of contact time on Rhodamine-B adsorption

The equilibrium time is one of the most important parameters in wastewater treatment systems. The results of the RhB adsorption capacity for the different lignocellulosic waste at different time intervals are depicted in Figure 2. Fast adsorption took place in the first 30 minutes, followed by a slower rate until equilibrium was reached after 120 min. The initial rapid adsorption could be attributed to the large number of sites available in the biosorbent for RhB molecules. However, the adsorption slowed down in later stages, since the remaining free sites on the surface of the biosorbent were more difficult to access. This same behavior has already been reported in the literature.[23,24] In view of these results, 120 minutes was taken as the equilibrium time for the remaining adsorption experiments for all materials.

The study of the adsorption kinetics may help to understand the mechanism controlling the adsorption, which depends on the physical and chemical characteristics of the adsorbent and the mass transfer process.[25] In this study, the adsorption rates were analyzed using pseudo-first order[26] and pseudo-second order models.[27]

The adsorption kinetics adjustments are shown in Figure 2, and all calculated kinetic parameters are summarized in Table 2. Correlation coefficients were closer to one for the pseudo-second order kinetic than for the pseudo-first order one for all materials. Furthermore, the adsorption capacity (q_{e_cal}) calculated from the pseudo-second order model was closer to the experimental value (q_{e_exp}). Hence, it can be concluded that the pseudo-second order kinetic model provides a good correlation, which is indicative of the fact that chemisorption (valence forces or electron exchange) is the limiting step.

Effects of initial concentration and temperature on Rhodamine-B absorption

Figure 3 shows an increase in the absorption capacity with increasing dye concentration. This increase was probably due to the increased driving force of the concentration gradient, which decreases the resistance to ion transfer between the aqueous medium and the sorbent.[28] On the other hand, the removal efficiency was higher at lower concentrations due to the high availability of active sites in comparison to the number of moles of the dye. Increased absorbance at higher temperatures was also observed, which suggested the endothermic nature of the process (see thermodynamic parameters discussion below). This can be attributed to an increase in the diffusion rate of the sorbate molecules, to changes in the sorbent porosity or to an increase in the availability of active sites.[29]

Adsorption isotherms describe how the molecules as distributed between the liquid phase and the surface of the solid phase. In the present study, the adsorption isotherms were simulated using the Langmuir[30] and Freundlich[31] models. The fittings of the experimental data to the Langmuir and Freundlich isotherm models at different temperatures are shown in Figure 3. All correlation coefficients (R^2) and the constants obtained from the application of both isotherm models are summarized in Table 3. The R^2 values, close to 1 for both isothermal models, indicated that they were reasonably good fits to the experimental data. The Langmuir isotherm model was a better fit for the experimental RhB absorption data for carnauba leaves and pine nut shell, which suggests that the dye was homogeneously adsorbed in a monolayer and that each dye molecule on the biosorbent surface had an activation energy.[32] Conversely, absorption on macauba endocarp showed a better fit to the Freundlich model, which may indicate that the dye was absorbed at different binding sites. The values of the n exponent in the Freunlich model were in the range of favorable adsorption ($1<n<10$) for all adsorbents. The maximum monolayer adsorption capacity values attained in this study were 36.54, 17.75 and 18.85 mg·g^{-1} for carnauba leaves, pine nut shell and macauba endocarp, respectively.

Thermodynamic parameters depend on the reaction process. The changes in the standard free energy (ΔG^0, kJ·mol^{-1}), in the standard adsorption enthalpy (ΔH^0, kJ·mol^{-1}) and in the standard absorption entropy (ΔS^0, kJ·mol^{-1}) were calculated using the absolute temperature in Kelvin and the Langmuir constant (mmol·g^{-1}). The thermodynamic parameters for the three materials are listed in Table 3. The negative ΔG^0 values for all materials indicated that the processes were spontaneous in nature. It is worth noticing that ΔG^0 values became more negative with increasing temperature, which indicates that the process became more spontaneous at higher temperatures. The enthalpy change value (ΔH) was positive for all the lignocellulosic materials, so the RhB sorption process was endothermic. Belala *et al.*,[24] who studied the adsorption of methylene blue onto date stones and palm-trees waste, also observed that the extent of adsorption steadily improved with an increase in adsorption temperature, due to an increased surface activity and an increased kinetic energy of dye molecules. Since the biosorption increased with temperature, therefore, the system was endothermic, in agreement with van't Hoff equation. Similar

observations have also been reported by Aksu and Tezer for Ramazol Black B adsorption on the green alga *Chlorella vulgaris*,[33] or for methylene blue on Guyava leaves[34] and sepiolite.[35] Further, the values below 40 kJ·mol⁻¹ suggest that the absorption had a physical contribution.[36] Lastly, the positive value of ΔS^0 suggests increased randomness at the solid/solution interface during the sorption of RhB for the various materials under study.

Liquid phase composition analysis after enzymatic hydrolysis of the lignocellulosic materials

The concentrations of total reducing sugars (TRS) are displayed in Table 4, together with the content of non-hydrolyzed material, HMF and furfural as fermentation inhibitors, and soluble lignin produced after enzymatic hydrolysis of the materials (before and after adsorption). TRS productions for lignocellulosic materials before adsorption were 42.86 g·L⁻¹ (85.72% yield), 38.19 g·L⁻¹ (76.38% yield) and 32.67 g·L⁻¹ (65.34% yield) for carnauba leaves, macauba endocarp and pine nut shell, respectively. These values were within the production ranges (21.3-83.1 g·L⁻¹) reported by Leaes *et al.*[37] and were higher than those presented by Kim *et al.*,[38] with ca. 20 g·L⁻¹, but would be susceptible of further improvement by means of sonication. TRS production from carnauba leaves and macauba endocarp after adsorption showed a slight decrease [37.84 g·L⁻¹ (75.68% yield) and 32.60 g·L⁻¹ (65.20% yield), respectively], while a slight increase was observed for pine nut shell (33.59 g·L⁻¹, 67.18% yield), which implies that these variations can be assigned to the influence of the matrix or the dye in the process of enzymatic hydrolysis.

Furan compounds are produced by direct dehydration of sugars in acidic conditions (caramelization) during thermal treatments.[39] In fact, under acidic conditions, 5-HMF can be produced even at low temperatures,[40] although its concentration significantly increases as the temperature of the thermal treatment is increased, or during long storage periods. Mohamed *et al.*[41] reported that the HMF content spontaneously increases at room temperature (RT) with time, with a monthly increase of 1.7 mg/kg for products with high sugars content (e.g. honey) and the magnitude of such increase remarkably varies depending on whether it is a cold or a hot region. Since our enzymatic hydrolysis assays were conducted in acidic conditions (pH 5), for three days (72 h), and at a temperature higher than RT (50 °C), a small production of furan compounds was expected, in agreement with Table 4. HMF presence was detected for C_{EH} (0.17 g·L⁻¹), C_{REH} (0.09 g·L⁻¹) and P_{REH} (0.03 g·L⁻¹) samples, while furfural was detected for M_{REH} (0.03 g·L⁻¹) and P_{REH} (0.01 g·L⁻¹) samples. These values were consistent with those reported by Chandler *et al.*,[42] who studied the acid hydrolysis of sugarcane bagasse, obtaining HMF values ranging from 0.047 to 0.276 g·L⁻¹. The presence of these compounds (furans) may have a deleterious effect on the fermentation process, in particular when yeasts are used.[43] Keating *et al.*[44] found that values beyond 0.06-0.08 g·L⁻¹ have inhibitory effects on the fermentation step. Thus, only for carnauba leaves after adsorption (C_{REH}) the furans concentration was above this limit (0.17 g·L⁻¹). Soluble lignin values indicated that the materials after absorption showed a better performance in delignification, with improved values for C_{EH} (32.1×10⁻³ g·L⁻¹), M_{EH} (23.6×10⁻³ g·L⁻¹) and P_{EH} (20.16×10⁻³ g·L⁻¹) samples, revealing that higher lignin removal was associated to higher TRS production. Therefore, the lignin content may also be an inhibitor of the enzymatic hydrolysis.[45] Kim *et al.*,[46] when studying the inhibitory effects of lignin, found that concentrations higher than 5 g/L had a negative impact on the enzymatic hydrolysis. Moreover, Ximenes *et al.*,[47] who studied the impact of phenolic compounds on the enzymatic hydrolysis of cellulose and cellobiose, also indicated that lignin had an inhibitory effect and specified that vanillin was the phenolic compound with the highest inhibitory effect.

For all samples, peaks corresponding to glucose, xylose, galactose, arabinose and fructose were identified. The highest sugars concentrations for the different materials were found for glucose (3.20 to 8.12 g·L⁻¹) and xylose (0.14 to 2.6 g·L⁻¹). This can be explained because glucose and xylose are the main constituents of cellulose and hemicellulose, respectively.[48] Lower concentrations were observed for galactose (0.05-0.16 g·L⁻¹), arabinose (0.01-0.12 g·L⁻¹) and fructose (0.21-1.22 g·L⁻¹) (see Table 4). The value attained for fructose could be attributed to the isomerization of glucose.

The sum of the sugars concentrations identified by ion chromatography diverged from the values of total reducing sugars. These later represent any sugar that either has an aldehyde group or that is capable of forming one in solution through isomerism, so all monosaccharides and most disaccharides (other than sucrose) are reducing sugars.[49] Therefore, aforementioned difference can be readily explained by the fact that ion chromatography only measures the major monosaccharides (glucose, xylose, galactose, arabinose and fructose).

CONCLUSION

The lignocellulosic materials under study behave as efficient biosorbents for Rhodamine-B (RhB) removal. The adsorption affinity for the different materials increases following the sequence: macauba endocarp > pine nut shell > carnauba leaves. The kinetic study fits a pseudo-second order kinetic model, which implies that chemisorption is the rate limiting step in the biosorption process. The materials require short periods of time to reach equilibrium (ca. 30 minutes), thus favoring their applicability to water treatment systems, since the retention times of the system would be decreased. On the other hand, the equilibrium data fits both Langmuir and Freundlich models, which suggests that both physical- and chemical-adsorption take place. Thermodynamic results show the feasible, spontaneous and endothermic nature of biosorption of RhB in the different studied materials.

With regard to the production of total reducing sugars (TRS) by enzymatic hydrolysis, the values attained were higher for raw materials than for the materials after the absorption treatment in the case of carnauba leaves and macauba shell (84wt% and 74.9wt%, respectively). Conversely, the production attained for pine nut shell was slightly higher after adsorption (65.9wt%). All in all, it can be concluded that these three materials show a good performance in the production of sugars after their use as biosorbents. This opens a new avenue for reuse and re-valorization of biomass from lignocellulosic residues by a combined use of two processes (enzymatic hydrolysis-biosorption) for water pollutants removal and subsequent fermentable sugars obtaining. Efforts are currently being undertaken to further improve TRS production yields by means of low-cost processes such as sonication. Both the effect of pretreatment prior to enzymatic hydrolysis and the impact of the adsorbed dye on the subsequent fermentation of TRS to obtain bioalcohols need to be assessed in future research.

REFERENCES

[1] P. O. Jones and P. T. Vasudevan, *Biotechnol. Lett*, **32**, 103 (2010).

[2] S. Ramakrishnan, J. Collier, R. Oyetunji, B. Stutts and R. Burnett, *Bioresour. Technol.*, **101**, 4965 (2010).

[3] K.-J. Wu, Y.-H. Lin, Y.-C. Lo, C.-Y. Chen, W.-M. Chen and J.-S. Chang, *J. Taiwan Inst. Chem. Eng.*, **42**, 20 (2011).

[4] P. Binod, K. Satyanagalakshmi, R. Sindhu, K. U. Janu, R. K. Sukumaran and A. Pandey, *Renewable Energy*, **37**, 109 (2012).

[5] S. González-García, M. T. Moreira and G. Feijoo, *Renew. Sust. Energ. Rev.*, **14**, 2077 (2010).

[6] J. D. D. Melo, L. F. M. Carvalho, A. M. Medeiros, C. R. O. Souto and C. A. Paskocimas, *Composites Part B*, **43**, 2827 (2012).

[7] D. d. C. Lopes, A. J. Steidle Neto, A. A. Mendes and D. T. V. Pereira, *Energy Economics*, **40**, 819 (2013).

[8] L. Balistrieri and J. W. Murray, *Am. J. Sci.*, **281**, 788 (1981).

[9] H. P. Boehm, *Carbon*, **32**, 759 (1994).

[10] R. Baccar, J. Bouzid, M. Feki and A. Montiel, *J. Hazard. Mater.*, **162**, 1522 (2009).

[11] R. Choudhary, A. L. Umagiliyage, Y. Liang, T. Siddaramu, J. Haddock and G. Markevicius, *Biomass Bioenergy*, **39**, 218 (2012).

[12] J. K. Lin, M. R. Ladisch, J. A. Patterson and C. H. Noller, *Biotechnol. Bioeng.*, **29**, 976 (1987).

[13] Q. Q. Wang, Z. He, Z. Zhu, Y. H. P. Zhang, Y. Ni, X. L. Luo and J. Y. Zhu, *Biotechnol. Bioeng.*, **109**, 381 (2012).

[14] R. Shrestha, A. Yadav, B. Pokharel and R. Pradhananga, *Res. J. Chem. Sci.*, **2**, 80 (2012).

[15] H. Zahir, M. Naidoo, R.-M. Kostadinova, K. A. Ortiz, R. Sun-Kou and A. E. Navarro, *Front. Environ. Sci.*, **2**, 1 (2014).

[16] N. Mosier, *Bioresour. Technol.*, **96**, 673 (2005).

17 E. Heredia-Olea, E. Perez-Carrillo, M. Montoya-Chiw and S. O. Serna-Saldivar, *Biomed Res Int*, **2015**, 325905 (2015).
18 G. L. Miller, *Analytical Chemistry*, **31**, 426 (1959).
19 C. Chi, Z. Zhang, H.-M. Chang and H. Jameel, *J. Wood Chem. Technol.*, **29**, 265 (2009).
20 L. Segal, J. Creely, A. Martin and C. Conrad, *Text. Res. J.*, **29**, 786 (1959).
21 M. C. Basso, E. G. Cerrella and A. L. Cukierman, *Ind. Eng. Chem. Res.*, **41**, 3580 (2002).
22 J. P. Mota and S. Lyubchik, "Recent Advances in Adsorption Processes for Environmental Protection and Security". Springer Netherlands, 2008, p.192.
23 P. D. Saha, S. Chakraborty and S. Chowdhury, *Colloids Surf. B. Biointerfaces*, **92**, 262 (2012).
24 Z. Belala, M. Jeguirim, M. Belhachemi, F. Addoun and G. Trouvé, *Desalination*, **271**, 80 (2011).
25 G. Tchobanoglous, F. L. Burton and H. D. Stensel, "Wastewater Engineering: Treatment and Reuse". 2003, p.1819.
26 S. Lagergren, "Zur Theorie der sogenannten Absorption gelöster Stoffe". PA Norstedt & söner, Stockholm, 1898, p.30.
27 Y.-S. Ho, "Absorption of heavy metals from waste streams by peat". University of Birmingham, Birmingham, United Kingdom, 1995.
28 Z. Aksu and G. Dönmez, *Chemosphere*, **50**, 1075 (2003).
29 R. Srivastava and D. C. Rupainwar, *Desalin. Water Treat.*, **11**, 302 (2009).
30 I. Langmuir, *J. Am. Chem. Soc.*, **40**, 1361 (1918).
31 H. Freundlich, "Über die Adsorption in Lösungen". Wilhelm Engelmann, Leipzig, 1906, p.98.
32 Y.-S. Ho, T.-H. Chiang and Y.-M. Hsueh, *Process Biochem.*, **40**, 119 (2005).
33 Z. Aksu and S. Tezer, *Process Biochem.*, **36**, 431 (2000).
34 D. K. Singh and B. Srivastava, *Indian J. Environ. Health*, **41**, 333 (1999).
35 M. Doğan, Y. Özdemir and M. Alkan, *Dyes Pigments*, **75**, 701 (2007).
36 A. Bhatnagar, E. Kumar, A. K. Minocha, B.-H. Jeon, H. Song and Y.-C. Seo, *Sep. Sci. Technol.*, **44**, 316 (2009).
37 E. X. Leaes, E. Zimmermann, M. Souza, A. P. Ramon, E. T. Mezadri, V. Dal Prá, L. M. Terra and M. A. Mazutti, *Biosys. Eng.*, **115**, 1 (2013).
38 D.-H. Kim, S.-B. Lee and G.-T. Jeong, *Bioresour. Technol.*, **161**, 348 (2014).
39 J. Guo, W. S. Xu, Y. L. Chen and A. C. Lua, *J. Colloid Interface Sci.*, **281**, 285 (2005).
40 T. Kawano, M. Kubota, M. S. Onyango, F. Watanabe and H. Matsuda, *Appl. Therm. Eng.*, **28**, 865 (2008).
41 F. S. Mohamed, W. A. Khater and M. R. Mostafa, *Chem. Eng. J.*, **116**, 47 (2006).
42 C. Chandler, N. Villalobos, E. González, E. Arenas, Z. Mármol, J. Ríos and C. A. Mazzarri, *Multiciencias*, **12**, 245 (2012).
43 D. Heer and U. Sauer, *Microb. Biotechnol.*, **1**, 497 (2008).
44 J. D. Keating, C. Panganiban and S. D. Mansfield, *Biotechnol. Bioeng.*, **93**, 1196 (2006).
45 B.-W. Koo, B.-C. Min, K.-S. Gwak, S.-M. Lee, J.-W. Choi, H. Yeo and I.-G. Choi, *Biomass Bioenergy*, **42**, 24 (2012).
46 Y. Kim, E. Ximenes, N. S. Mosier and M. R. Ladisch, *Enzyme Microb. Technol.*, **48**, 408 (2011).
47 E. Ximenes, Y. Kim, N. Mosier, B. Dien and M. Ladisch, *Enzyme Microb. Technol.*, **46**, 170 (2010).
48 V. C. Coletta, C. A. Rezende, F. R. da Conceição, I. Polikarpov and F. E. G. Guimarães, *Biotechnol. Biofuels*, **6**, 43 (2013).
49 J. M. Berg, J. L. Tymoczko and L. Stryer, "Biochemistry", 7th ed. W.H. Freeman, New York, 2012, p.1054.

Table 1. Physical properties and chemical-adsorption characteristics of the materials under study

Properties	Carnauba leaves	Macauba endocarp	Pine nut shell
Elementary analysis (wt%)			
Carbon	45.4	52.6	47.7
Hydrogen	2.5	5.9	6.6
Nitrogen	3.4	0.3	0.3
Oxygen[a]	48.7	41.2	45.4
Surface groups (mmol$\cdot$g^{-1})			
Carboxylic	0.483	0.643	0.322
Lactonic	0.079	0.080	0.162
Phenolic	2.981	2.820	2.735
Carbonylic	0.325	0.160	0.323
Total acidic	3.869	3.704	3.541
Basic	0.66	0.22	0.33
Total groups	4.529	3.924	3.844
BET specific surface area (m$^2\cdot$g^{-1})	0.8581	0.6028	0.8608
Mean pore diameter Dp (nm)	2.1246	13.39933	14.6974
Total pore volume (cm$^3\cdot$g^{-1})	0.00359	0.002019	0.00316
Iodine number (mg$\cdot$g^{-1})	523.86	367.31	413.59
Methylene Blue index (mg$\cdot$g^{-1})	978.37	922.54	857.83
pH$_{pzc}$	5.5	4.0	4.3

[a] Calculated by subtraction.

Table 2. Kinetic parameters for absorption of RhB onto different materials

Samples	C_0 (mg$\cdot$L^{-1})	q_{e_exp}	Pseudo-first order model			Pseudo-second order model		
			k_1 (min)	q_{e_cal} (mg$\cdot$g^{-1})	r^2	k_2 (g$\cdot$mg$^{-1}\cdot$min^{-1})	q_{e_cal} (mg$\cdot$g^{-1})	r^2
Carnauba leaves	5	2.29	0.328	2.152	0.996	0.3457	2.208	0.998
Macauba endocarp	20	9.81	0.2818	9.521	0.995	0.057	9.852	0.999
Pine nut shell	5	1.89	0.161	1.706	0.964	0.1294	1.823	0.989

Table 3. Isotherm parameters for Rhodamine B (RhB) biosorption onto different materials

Samples		Carnauba leaves			Macauba endocarp			Pine nut shell		
T (ºC)		25	35	45	25	35	45	25	35	45
Langmuir constants	q_{max} (mg$\cdot$g^{-1})	27.917	30.162	36.541	16.164	16.705	17.75	17.325	18.621	18.855
	K_L (L$\cdot$mg^{-1})	0.1160	0.1182	0.1194	2.0565	2.8016	2.8996	0.0471	0.0481	0.0530
	r^2	0.994	0.988	0.992	0.975	0.977	0.976	0.980	0.998	0.998
Freundlich constants	K_F (mg$\cdot$g^{-1} (mg$\cdot$L^{-1})$^{1/n}$)	3.111	3.366	4.032	9.501	11.221	12.394	1.025	1.138	1.301
	n	1.393	1.367	1.314	2.689	3.086	2.730	1.397	1.406	1.452
	r^2	0.978	0.979	0.986	0.983	0.995	0.991	0.968	0.994	0.998
Thermodynamic parameters	ΔG^0 (kJ$\cdot$mol^{-1})	-9.923	-10.304	-10.665	-17.046	-18.409	-19.098	-7.689	-8.001	-8.517
	ΔH^0 (kJ$\cdot$mol^{-1})	1.141			13.646			4.615		
	ΔS^0 (J$\cdot$mol$^{-1}\cdot$K^{-1})	37.138			103.351			4.953		
	r^2	0.977			0.838			0.866		

Table 4. Liquid phase composition after the enzymatic hydrolysis of the different materials, before and after adsorption

Sample	TRS		HMF (g·L⁻¹)	Furfural (g·L⁻¹)	Soluble lignin (mg·L⁻¹)	Monosaccharides (ion chromatography) (g·L⁻¹)				
	(g·L⁻¹)	%				Glucose	Xylose	Galactose	Arabinose	Fructose
C_{EH}	42.86	85.72	0.17	0.00	32.10	3.64	0.14	0.16	0.12	0.63
C_{REH}	37.84	75.68	0.09	0.00	25.54	3.20	0.13	0.12	0.09	0.59
M_{EH}	38.19	76.38	0.00	0.00	23.60	4.17	2.58	0.06	0.03	0.66
M_{REH}	32.60	65.20	0.00	0.03	14.12	3.47	1.20	0.05	0.01	0.21
P_{EH}	32.67	65.34	0.00	0.00	20.16	4.22	0.24	0.07	0.03	0.66
P_{REH}	33.59	67.18	0.03	0.01	12.70	8.18	0.37	0.13	0.04	1.22

C_{EH}: carnauba leaves after enzymatic hydrolysis; C_{REH}: carnauba leaves with RhB after enzymatic hydrolysis; M_{EH}: macauba endocarp after enzymatic hydrolysis; M_{REH}: macauba endocarp after enzymatic hydrolysis; P_{EH}: pine nut shell after enzymatic hydrolysis; P_{REH}: pine nut Shell with RhB after enzymatic hydrolysis.
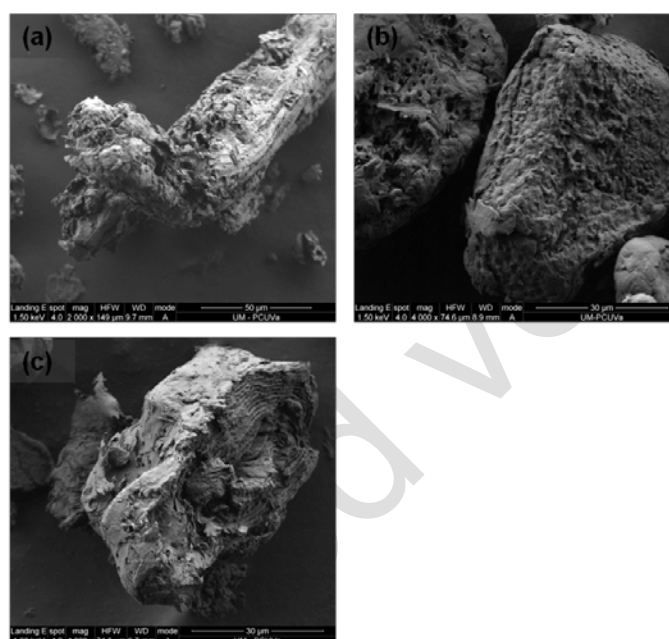

Figure 1. Scanning electron micrographs of the three raw materials: (a) carnauba leaves; (b) macauba endocarp; and (c) pine nut shell.
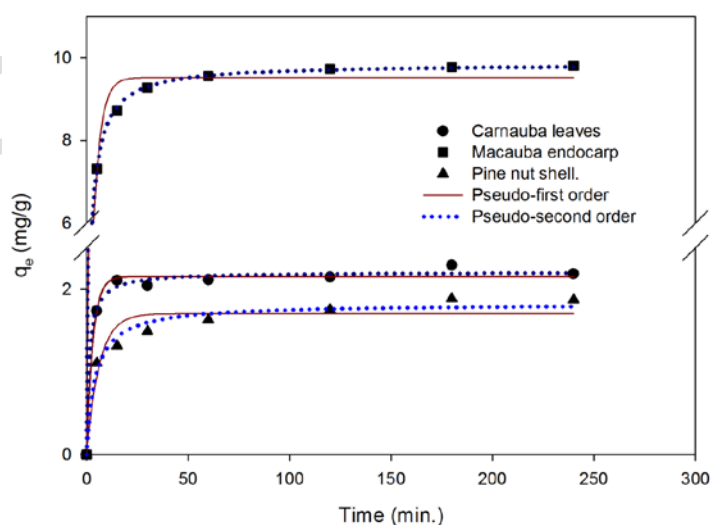

Figure 2. Effect of contact time on the absorption of RhB onto different materials (natural pH, temperature 25±5ºC)
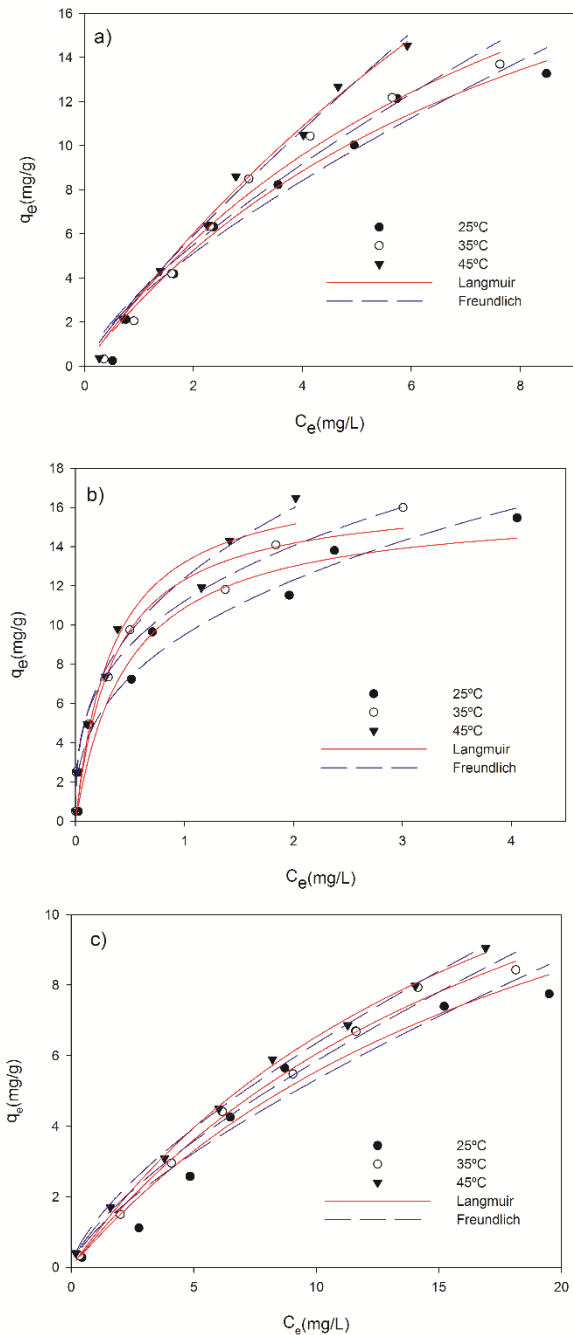
9

Figure 3. Equilibrium isotherms for Rhodamine B (RhB) at different temperatures (25ºC, 35ºC and 45ºC) onto: (*a*) carnauba leaves; (*b*) macauba endocarp; and (*c*) pine nut shell. Red solid lines represent the fitting curves using the Langmuir model and Freundlich model fittings are represented as dashed blue lines.